Shi *et al. Cell Communication and Signaling* (2025) 23:152
https://doi.org/10.1186/s12964-025-02158-3

Cell Communication and Signaling

RESEARCH Open Access

Exosome-transmitted HSPA9 facilitates bortezomib resistance by targeting TRIP13/USP1 signaling in multiple myeloma

Min Shi[1], Na Shen[1], Xiangyu Liu[1], Jiapei Yu[1], Xuxing Shen[1], Ying Chen[1], Yuan Xia[1] and Lijuan Chen[1*]

Abstract

Background Resistance to the proteasome inhibitor bortezomib (BTZ) poses a formidable therapeutic challenge in multiple myeloma (MM). Our study aims to analyze the mechanism by which exosomes heat shock 70 kDa protein 9 (HSPA9) secreted by BTZ-resistant MM cells disseminate resistance to BTZ-sensitive MM cells.

Methods The serum exosomes were identified by nanoparticle tracking analysis and transmission electron microscopy. Liquid chromatography-mass spectrometry and public databases were performed to screen exosomes HSPA9. Cell counting kit-8, western blotting and colony formation assay were used to detected the role of HSPA9 protein in vitro. Co-immunoprecipitation, immunofluorescence and protein truncation test experiments were used to determine the regulatory network of the HSPA9-USP1-TRIP13 complex. Optical imaging in vivo and xenograft mouse models were performed to investigate that exosomes HSPA9 promoted MM proliferation and BTZ resistance.

Results We demonstrated that HSPA9 was highly expressed in serum exosomes and BTZ-resistant MM patients. Knockdown of HSPA9 significantly suppressed tumorigenesis and reversed BTZ resistance in vitro. As a downstream molecular of HSPA9, thyroid hormone receptor-interacting protein 13 (TRIP13) was also highly expressed in BTZ-resistant MM patients. Mechanistically, the carboxyl-terminal peptide-binding domain of HSPA9, provides a platform for recruiting the deubiquitinating enzyme ubiquitin-specific peptidase 1 (USP1), which prevents TRIP13 protein degradation. The HSPA9-USP1-TRIP13 complex exhibits stability in the cytoplasm, and its inhibition remarkably enhances BTZ resistance *in vito*.

Conclusion Our findings propose a pioneering molecular regulatory network in which MM-cell-derived exosomes HSPA9 transmitted BTZ resistance through the USP1/TRIP13 signaling pathway. This research highlights exosomes HSPA9 as a promising target to overcome MM BTZ resistance.

Plain English Summary

Bortezomib (BTZ) is a proteasome inhibitor used to treat multiple myeloma (MM), however, resistance to BTZ poses a formidable challenge in MM treatments and the underlying mechanisms remain poorly understood. In this study, we demonstrated that the heat shock 70 kDa protein 9 (HSPA9) was highly expressed in the serum exosomes of BTZ-resistant MM patients and cell lines. Elevated levels of HSPA9 promoted disease progression, poor prognosis,

*Correspondence:
Lijuan Chen
chenljb@126.com

Full list of author information is available at the end of the article

cell proliferation, BTZ resistance and stemness characteristics in MM. In addition, exosomes HSPA9 secreted by BTZ-resistant MM cells can disseminate BTZ resistance characteristics to BTZ-sensitive MM cells via endocytosis and activated drug resistance signaling pathways at the same time. Mechanistically, the carboxyl-terminal peptide-binding domain of HSPA9 provided a platform for recruiting a deubiquitinating enzyme named ubiquitin-specific peptidase 1 (USP1), which could prevent thyroid hormone receptor-interacting protein 13 (TRIP13) protein from degradation. The HSPA9-USP1-TRIP13 complex exhibits stability in the cytoplasm, and its inhibition rendered MM cells more sensitive to BTZ treatment. Consequently, our findings propose a pioneer molecular regulatory network in which MM-cell-derived exosomes HSPA9 can transmit BTZ resistance through the USP1/TRIP13 signaling pathway. This research highlights exosomes HSPA9 as a promising therapeutic target to overcome BTZ resistance in MM.

Keywords Exosome, HSPA9, Multiple myeloma, USP1, TRIP13

Introduction

As the second common hematologic malignancy, multiple myeloma (MM) is a bone marrow neoplastic disease characterized by uncontrolled proliferation of malignant plasma cells [1, 2]. Recently, tremendous advances have been made in the molecular and cytogenetic mechanisms of MM pathogenesis. But MM is still a devastating disease caused by inevitable occurrence of drug resistance after tumor heterogeneity and clonal evolution [3, 4]. Bortezomib (BTZ) is a first-line selective proteasome inhibitor (PI) in MM treatment, and BTZ resistance is one of the main obstacles in the treatment of MM [5]. Therefore, it is urgent to elucidate the mechanism of BTZ resistance and discover novel therapeutic targets for MM treatment.

Exosomes are nano-sized vesicles, with a diameter ranging from 30 to 150 nm. Accumulating studies have shown that exosomes play vital biological functions in the human body. Tumor-derived exosomes play an integral role in cancer-stroma crosstalk by transmitting a variety of informational cargo into the extracellular microenvironment [6, 7], resulting in cancer development, immune escape, and tumor drug resistance [8–12]. However, the molecular mechanism of how exosomes precipitate myeloma cells became resistant to BTZ is unexplored, and whether exosomes from BTZ-resistant cells could confer BTZ resistance to BTZ-sensitive MM cells needs to be further clarified.

Heat shock response is characterized by cell protection and is accountable for synthesizing heat shock proteins [13]. These HSPs participate in the correct folding of newly synthesized proteins as molecular chaperones, assist in refolding abnormally folded proteins, and coordinate with the ubiquitin-proteasome system to regulate the degradation of misfolded proteins [14, 15]. Heat shock 70 kDa protein 9 (HSPA9) belongs to the HSP70 family, and elevated expression of HSPA9 is observed in a variety of tumors, contributing to the tumor proliferation and growth [16, 17]. Ferguson et al. [14] analyzed the transcriptome data of 773 newly diagnosed multiple myeloma (NDMM) patients from China in the CoMMpass database. They found that HSPA9 was associated with poor outcomes in NDMM patients and maintained protein homeostasis. High HSPA9 expression in MM patients dramatically increased the possibility of PIs resistance, but the molecular mechanism was rarely investigated or reported.

Ubiquitination and deubiquitination are essential and very common post-translational modification (PTM) processes [18]. Increasing evidence indicated that inhibitory compounds targeting groups of ubiquitin-deubiquitination can stabilize protein degradation levels [19]. and play a vital role in overcoming MM therapy resistance [20]. Ubiquitin-specific peptidase 1 (USP1) belongs to the deubiquitinating enzyme (DUB) family and maintains genomic stability by deubiquitinating specific cellular substrates [21]. Previous studies discovered that blocking USP1 inhibited the ability of MM cells to repair damaged DNA and subsequently induced cell apoptosis, indicating the anti-tumor activity of USP1 in MM cells [22, 23]. However, the precise function and the underlying molecular mechanism of USP1 in MM disease and drug resistance have not been fully clarified.

Thyroid hormone receptor-interacting protein 13 (TRIP13), which belongs to the ATPases associated with diverse cellular activities (AAA) protein family [24], has been demonstrated to play a role in oncogenic processes [25] and chromosome-related processes [26]. TRIP13 is one of 70 genes overexpressed in high-risk MM [27] and one of 10 genes that promote MM chromosomal instability features in MM [28]. Previous research indicated that TRIP13 facilitated the progression of B-cell lymphoma [29] and enhanced MM stemness phenotype and resistance to BTZ [30]. Therefore, it is warranted to investigate the probable role of TRIP13 in triggering MM tumorigenesis and PIs drug resistance.

In the present study, we analyzed the differentially expressed proteins (DEPs) in serum exosomes derived from BTZ-sensitive and BTZ-resistant MM samples and found that exosomes HSPA9 mediated BTZ resistance. Our findings highlighted that exosomes HSPA9 could target a panel of clonal myeloma cells and transmit BTZ

resistance information to BTZ-sensitive cells via the USP1/TRIP13 pathway. It set up the theoretical foundation for finding a therapeutic route to overcome MM treatment resistance from a new perspective and has the potency to improve MM clinical treatment efficacy.

Materials and methods

Cell culture

Human U266 and RPMI8226 MM cell lines were maintained in RPMI-1640 medium (Gibco, USA). HEK-293T cell line was cultured in DMEM. The RPMI8226 cell line was selected as the induction target. A dose escalation method was employed to increase the BTZ drug concentration, starting from 1nM and incrementing by 1nM at each step. When cell growth decelerated, the medium was replaced with BTZ-free medium to allow cell recovery. After the cells regained their normal state, the aforementioned steps were repeated for intermittent induction over a period exceeding six months. The CCK-8 assay was used to detect the half-maximal inhibitory concentration of RPMI8226 drug-resistant cell lines, and the IC50 was 34.30 ± 2.69 nM. All the cell lines obtained from the ATCC, were maintained with 10% fetal bovine serum and 1% penicillin/streptomycin at 37 °C and 5% CO_2.

Patients

Patients with MM admitted to the First Affiliated Hospital of Nanjing Medical University between December 2017 and August 2018 were enrolled in this study. All MM patients were diagnosed according to IMWG 2014 criteria [31]. Enrolled participants were divided into BTZ-sensitive group, BTZ-resistant group and healthy donor (HD) group. Serum samples were obtained from each participant.

Exosome isolation

The supernatant from cell culture medium containing exosomes and floating cells was extracted using an exosome kit according to the experimental procedure (Plasma/Serum Exosome Purification Kits, Canada). We extracted the medium of HEK293T and HEK293T-HSPA9-OE cells (1×10^7) to obtain cell-derived exosomes using ultracentrifugation for more experiments.

Exosome staining and in vivo optical imaging

According to the procedure established by the reagent manufacturer, the exosomes were labeled with the fluorescent dye PKH26 (MX4021, Maokangbio). Subsequently, the PKH26-labeled exosomes were appended to the cell lines or injected into the mice through the tail vein. Exosomal bioluminescence imaging was performed and quantified using IVIS Spectrum (PerkinElmer, USA) in mice at different times.

Drug sensitivity analysis

Drug sensitivity analysis of GSE2658 was performed using the oncopredict package. The Wilcoxon test was employed to ascertain the BTZ sensitivity between the expression of HSPA9-high and HSPA9-low groups. The relationship of HSPA9 expression to BTZ sensitivity was investigated through the utilisation of Spearman correlation analysis.

Analysis of transcriptomics data

Three public available datasets (GSE2658, GSE5900 and GSE31161) were downloaded and integrated. These data were normalized using the normalizeBetweenArrays function in the limma package. The integrated dataset contains 637 samples from HD, monoclonal gammopathy of undetermined significance (MGUS), smoldering multiple myeloma (SMM) and MM patients in GSE2658 and GSE5900. MM patients included 1038 samples at baseline, and relapse were obtained from GSE31161. All samples were included for downstream analysis. Statistical analyses for comparison between multiple groups were performed using the Kruskal-Wallis test.

Transmission electron microscopy (TEM)

The prepared 20μL exosomes were pipetted onto copper grids with adsorption for 20 min, and stained with 2% phosphotungstic acid solution at room temperature for 1 min. Images of exosomes were obtained by transmission electron microscope (FEI Tecnai 12, Philips).

Nanoparticle tracking analysis (NTA)

Isolated exosomes were filtered with a 0.22 μm filter and diluted 100-fold to a concentration of 10^8 particles/mL with PBS. The size and concentration of exosomes were determined using the NanoSight NS 300 system (NanoSight Technology, UK).

Survival analysis

Data integration was performed by sva. We used the log-rank test provided by the R packages "survminer" to analyze survival in GSE2658 and GSE24080. Based on the expression of HSPA9, samples were divided into HSPA9-high and HSPA9-low groups, and the optimal cutoff point was obtained using the surv_cutpoint function in survminer.

MM xenograft mouse model

BALB/c nude mice (male, 6-week-old) were obtained from Gempharmatech Co., Ltd (Nanjing, China). RPMI 8226 cells (100 μl PBS containing 5×10^6 cells) were injected subcutaneously into the underarm of each mouse. After 7 days, mice were randomly divided into 6 groups and treated with the following drugs twice a week. Control group: PBS, i.v., 100 μl/mouse; BTZ group:

BTZ, i.H., 0.5 mg/kg; exosome group: exo-HSPA9, i.v., 30 μg/mouse; BTZ + exosome group: BTZ, i.H., 0.5 mg/kg + exo-HSPA9, i.v., 30 μg/mouse; ML323 group: ML323, i.p., 5 mg/kg; ML323 + exosome group: ML323, i.p., 5 mg/kg + exo-HSPA9, i.v., 30 μg/mouse). The mice weight and tumor diameter were measured before each injection. Following a 21-day treatment, the mice were euthanized and the weight of each group was quantified. Part of the mouse tumors in each group were used for HSPA9 and Ki-67 IHC staining. The rest were fixed with 4% paraformaldehyde for follow-up experiments.

Supplemental methods

Liquid chromatography-Mass spectrometry (LC-MS/MS) analyses, protein identification and quantification, functional enrichment analysis, cell viability and apoptosis assay, constructing plasmid and cell transfection, immunohistochemistry, quantitative real-time reverse transcriptase-polymerase chain reaction (qRT-PCR), colony formation assay, immunofluorescence (IF), western blotting (WB) and co-immunoprecipitation (co-IP), in vitro ubiquitination assay are provided in Supplementary Materials.

Statistical analysis

The data pertaining to the experimental groups was performed using GraphPad Prism software (version 8.0), with the results presented as mean ± SD. Unpaired Student's t-test and one-way ANOVA test were used to compare the differences between groups. Kaplan-Meier curve was used for survival analysis, while the Log-rank method was utilized for the significance test. A P-value < 0.05 was statistically significant.

Results

Extraction and identification of serum exosomes in patients

To get insights into the potential advancement of MM, serum exosomes were extracted from patients in the HD, BTZ-sensitive and BTZ-resistant groups. The sizes of obtained exosome vesicles were measured by NTA, which were found to be in the range of 10–100 nm (Fig. 1A). The morphology and characteristics of the isolated exosomes were observed via TEM, revealing that the exosomes were cup-shaped spheres (Fig. 1B). These results confirm that the vesicles extracted from serum samples were exosomes.

Exosomes HSPA9 and HSPA9 protein are implicated in MM resistance to BTZ

To screen for DEPs, protein mass spectrometry analysis was performed on 8 pairs of serum exosomes in the HD, BTZ-sensitive and BTZ-resistant groups (Fig. 1C). After the removal of common high-abundance proteins, 193 and 234 proteins were identified in the BTZ-sensitive and BTZ-resistant groups, respectively. Compared to the BTZ-sensitive group, there were 12 up-regulated and 8 down-regulated DEPs in the BTZ-resistant group. Among the up-regulated proteins, we found that the heat shock protein HSPA9 exosomes were significantly upregulated in the BTZ-resistant group ($P = 0.04$) (Fig. 1D), indicating that HSPA9 involved in MM. To validate this hypothesis, we first detected the level of HSPA9 exosomes using WB analysis. We found that compared with BTZ-sensitive samples ($n = 11$), the expression of exosomes HSPA9 protein was significantly elevated in BTZ-resistant samples ($n = 11$) (Fig. 1E and Supplementary Fig. S2). Density quantitative analysis showed that exosomes HSPA9 protein were significantly highly expressed in BTZ-resistant samples ($P = 0.0095$) (Fig. 1F). Additionally, we enriched exosomes in the culture supernatants of RPMI8226-DR and RPMI8226-WT cell lines and found that more exosomes HSPA9 protein were secreted in RPMI8226-DR cells compared to the control group (Fig. 1G). According to the NDMM cases in the GSE2658 database, the sensitivity to BTZ was negatively correlated with the mRNA level of HSPA9 ($P < 0.001$) (Fig. 1H). Data from the GSE5900 and GSE2658 databases indicated a progressive increase in HSPA9 expression levels correlating with the advancement of MM ($P < 0.001$) (Fig. 1I). Moreover, the expression level of HSPA9 was negatively correlated with overall survival (OS) in MM patients ($P = 0.015$) (Fig. 1J). To explore the clinical significance of HSPA9, we collected bone marrow biopsy tissues from BTZ-sensitive ($n = 20$) and BTZ-resistance ($n = 20$) MM patients for immunohistochemical (IHC) analysis. The staining results revealed that the expression of HSPA9 was significantly upregulated in the BTZ-resistance group ($P < 0.0001$), and HSPA9 was predominantly localized in the cytoplasm and membrane of tumor cells (Fig. 1K-L). Therefore, we speculate that exosomes HSPA9 and HSPA9 protein are relevant to BTZ resistance in MM, and high expression of HSPA9 deteriorated MM disease progression.

HSPA9 protein accelerates MM cell proliferation, BTZ resistance and stemness characteristics in vitro

Compared with MM cells, isolation and extraction of exosomes from tool cells HEK 293T is a more efficient process, and these exosomes have the advantages of high yield, stability and purity. To interrogate the biological behavior of HSPA9 and its involvement in BTZ resistance, we knocked down and overexpressed HSPA9 (HSPA9-KD and HSPA9-OE) in MM cells (RPMI8226 and U266) using a lentiviral vector, and verified the knockdown efficiency by WB assay (Fig. 2A). Cell counting kit-8 (CCK-8) assay showed that the proliferation activity of HSPA9-KD MM cells was significantly inhibited in a time-dependent

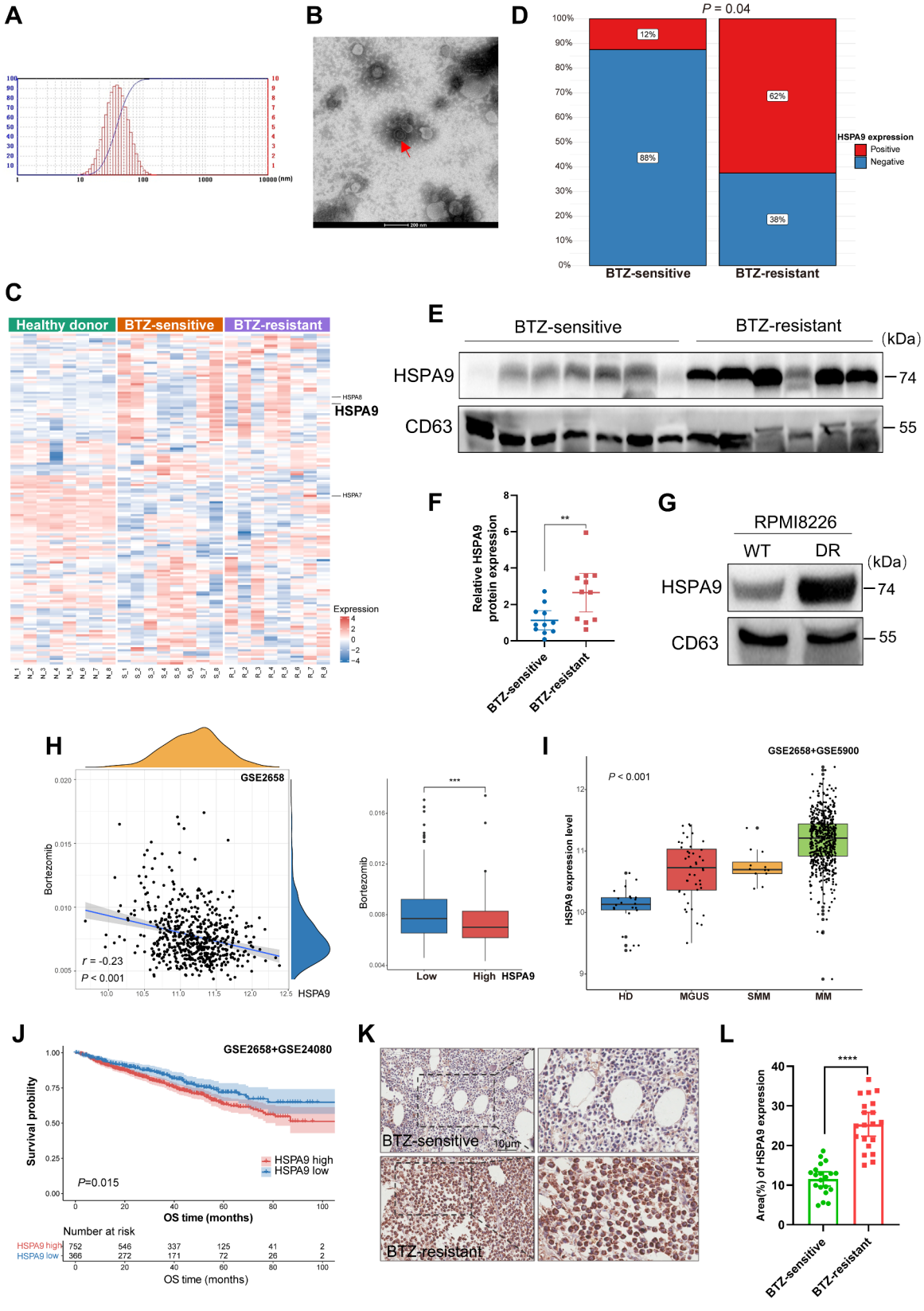

Fig. 1 (See legend on next page.)

(See figure on previous page.)

Fig. 1 Exosomes HSPA9 and HSPA9 protein are highly expressed in BTZ-resistant MM. NTA (**A**) and transmission electron microscopy (**B**) verified the size and structure of exosomes. Red arrows indicated exosomes morphology. Scale bar, 200 nm. (**C**) The DEPs heatmaps of serum exosomes in 8 pairs of HD/MM patients. (**D**) The expression of exosomes HSPA9 in BTZ-sensitive and BTZ-resistant MM patients ($P = 0.04$). (**E**-**F**) WB analysis and densitometric quantification of the expression of exosomes HSPA9 protein in MM patients ($P = 0.0095$). (**G**) Exosomes HSPA9 protein were highly expressed in RPMI8226 BTZ-resistant MM cells. (**H**) BTZ sensitivity was negatively correlated with HSPA9 mRNA expression in GSE2658 ($P < 0.001$). High expression of HSPA9 was associated with MM (**I**) progression and (**J**) poor OS ($P < 0.001$ and $= 0.015$, respectively). (**K**-**L**) The expression of HSPA9 protein in bone marrow IHC from BTZ-sensitive and BTZ-resistance MM patients ($P < 0.0001$). *$P < 0.05$; **$P < 0.01$; ***$P < 0.001$; ****$P < 0.0001$

manner compared to the control group (Fig. 2B). Subsequently, under the intervention of BTZ at different doses and times, the IC_{50} was (6.72 ± 0.14) nM, (4.57 ± 0.42) nM, (8.63 ± 0.19) nM and (6.24 ± 0.20) in RPMI8226-Scr and RPMI8226-HSPA9-KD, U266-Scr and U226-HSPA9-KD cells at 24 h, respectively. The results indicated that the knockdown of HSPA9 enhanced the sensitivity of MM cells to BTZ in a dose- and time-dependent manner (Fig. 2C-D). Flow cytometry demonstrated that the apoptosis of the HSPA9-KD cells increased after BTZ treatment for 24 h, indicating that MM cells exhibited heightened sensitivity to BTZ after knockdown of HSPA9 (Fig. 2E). Notably, BTZ treatment induced remarkable apoptosis of the HSPA9-KD MM cells, which was related to the protein of cleaved caspase 3 (Fig. 2F). Colony-formation assay showed that the colonies of the HSPA9-OE MM cells increased in both morphology and number ($P = 0.0014$) (Fig. 2G and Supplementary Fig. S3). In addition, the expression of NANOG, OCT4 and SOX2, three markers representing induced pluripotent or embryonic stem cell (iPS/ES), was elevated in the RPMI8226 and U266 HSPA9-OE MM cells (Fig. 2H). These data imply that the knockdown of HSPA9 attenuated MM proliferation and encouraged apoptosis, and HSPA9 promotes MM cell BTZ resistance and maintains stemness characteristics in *vitro*.

Exosomes HSPA9 derive from BTZ-resistant cells disseminate drug resistance characteristics to sensitive cells

Given that exosomes HSPA9 are involved in BTZ resistance, we are eager to clarify if exosomes derived from BTZ-resistant cells could alter the characteristics of BTZ-sensitive cells. HEK293T cells were infected with HSPA9-OE lentiviral vectors, and the efficiency was verified by WB (Fig. 3A). To obtain exosomes HSPA9-OE secreted by HEK 293T cells, they were extracted using the differential centrifuge method. The result showed that the extracted vesicles contained high concentrations of CD81 and Alix-labeled proteins (Fig. 3B).

As demonstrated by the CCK-8 assay, the addition of exosome HSPA9-OE (10 μg/mL) to MM cells could reverse the inhibition of cell proliferation resulting from HSPA9 knockdown (Fig. 3C). In follow-up studies, after adding exosome HSPA9-OE (10 μg/mL) into HSPA9-KD MM cells (RPMI8226 and U266) treated with BTZ (5nM), we were surprised to find those exosome HSPA9-OE could induce HSPA9-KD MM cells to regain BTZ resistance (Fig. 3D).

To investigate the potential mechanism of this phenomenon, we added exosomes HSPA9 (10 μg/mL) to HSPA9-KD MM cell lines (RPMI8226 and U266) and detected the expression level of HSPA9 by WB (Fig. 3E) and qRT-PCR (Fig. 3F). These findings strongly revealed that exosomes HSPA9 could not reverse the expression of HSPA9 at the protein level, but could reverse it at the RNA level. To trace exosomes, we first co-cultured flag-labeled RPMI8226-HSPA9-OE and RPMI8226-WT cells for 24 h aiming to observe the production of endogenous exosomes labeled with PKH26. Confocal laser scanning microscope (CLSM) images illustrated that the Flag and PKH26-labeled exosomes HSPA9 were tracked in RPMI8226-WT cells (Fig. 3G). Secondly, we added PKH26-labeled exosomes HSPA9 to RPMI8226-WT and U266-WT cells in the extracellular space. Importantly, it was found that the number of red fluorescently labeled exosome HSPA9 gradually increased with time in the intracellular (Fig. 3H). In summary, BTZ-sensitive MM cells acquire resistance via internalizing the exosomes HSPA9 released from BTZ-resistant cells. This process of resistance transmission is regulated at both the mRNA and protein level.

The molecular chaperone HSPA9 protein is positively regulating TRIP13

To unveiled the mechanisms by which HSPA9 exerts BTZ resistance in MM, we performed immunoprecipitation binding mass spectrometry (IP-MS) in RPMI8226-WT cells to screen potential proteins that interacted with HSPA9 (Fig. 4A). TRIP13, which encodes a protein that interacts with thyroid hormone receptors, emerged as a prime candidate and caught our attention (Fig. 4B-C). To examine the relationship between HSPA9 and TRIP13, we utilized the co-immunoprecipitation (co-IP) assay and confirmed the interaction between the two proteins (Fig. 4D). In addition, TRIP13 expression was significantly decreased in RPMI-8226 and U226 cells with HSPA9 knockdown (Fig. 4E), while increased in RPMI8226 and U226 cells with HSPA9 overexpression (Fig. 4F). Following the transfer of the TRIP13-OE plasmid into RPMI8226-WT and U226-WT cells, the expression of HSPA9 was not significantly changed (Fig. 4G). CLSM images showed that HSPA9 and TRIP13 were co-localized in the cytoplasm of RPMI8226-WT and

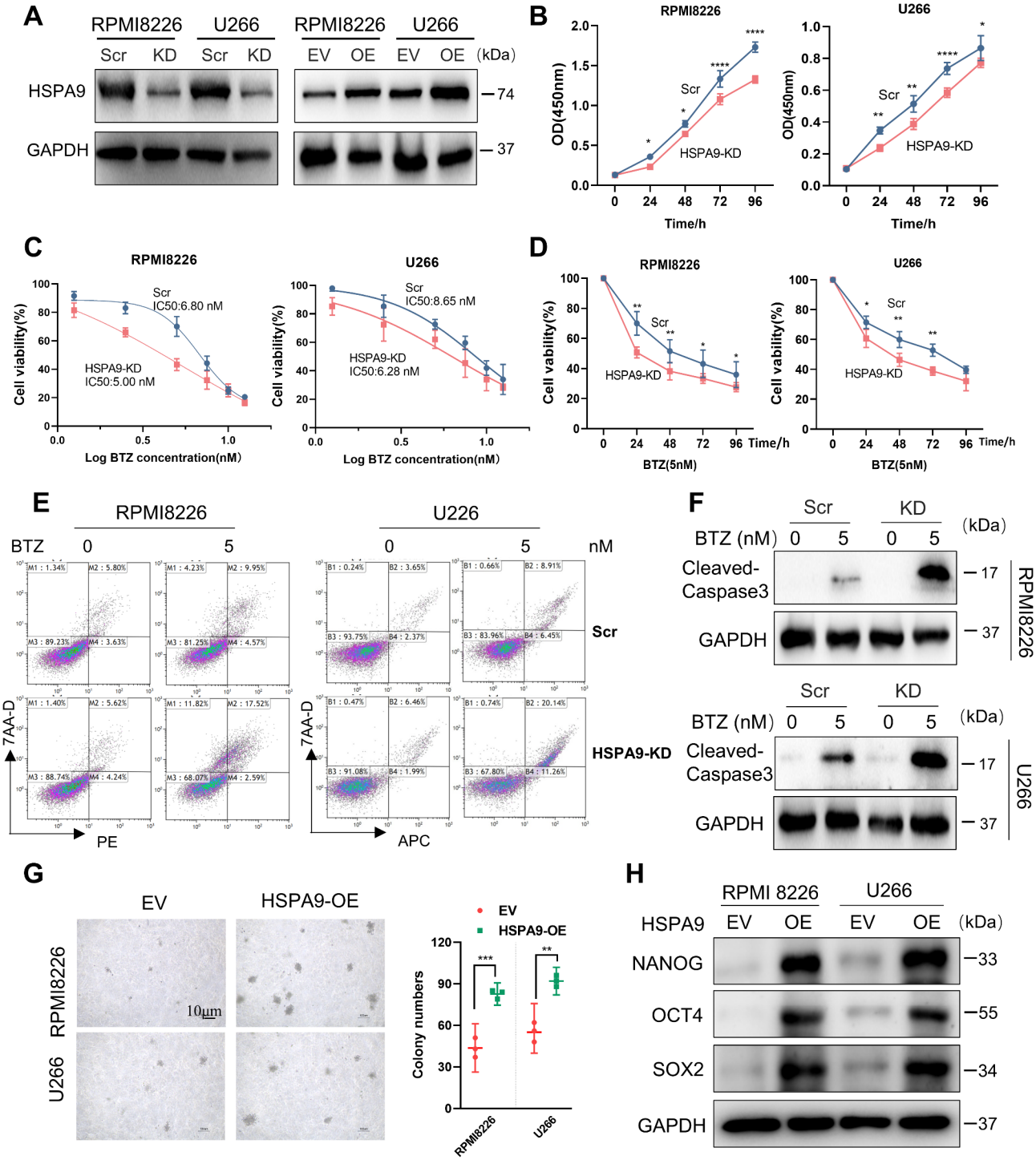

Fig. 2 HSPA9 protein promotes MM cell proliferation, BTZ resistance and stemness characteristics in vitro. (**A**) WB assay detected the efficiency in the HSPA9-KD and HSPA9-OE MM cells (RPMI8226 and U266). (**B**) CCK-8 assay detected the cell growth viability in the HSPA9-KD MM cells. (**C**) CCK-8 assays assessed the viability of MM cells after treatment with dose concentrations of BTZ for 24 h. (**D**) CCK-8 assays assessed the viability of MM cells after treatment with the 5nM concentration of BTZ for 96 h. (**E**) Flow cytometry detected the apoptosis of MM cells after BTZ treatment for 24 h. (**F**) WB detected the apoptosis of cleaved-caspase3 proteins after BTZ treatment for 24 h. (**G**) Representative images of soft agar colony formation and the colony numbers of each group ($P = 0.0014$) in the MM cells. Scale bar, 10 μm. (**H**) WB analysis showed pluripotent markers expression of NANOG, SOX2, and OCT4 in HSPA9-OE MM cells. Data are presented as the mean ± SD. *$P < 0.05$; **$P < 0.01$; ***$P < 0.001$; ****$P < 0.0001$

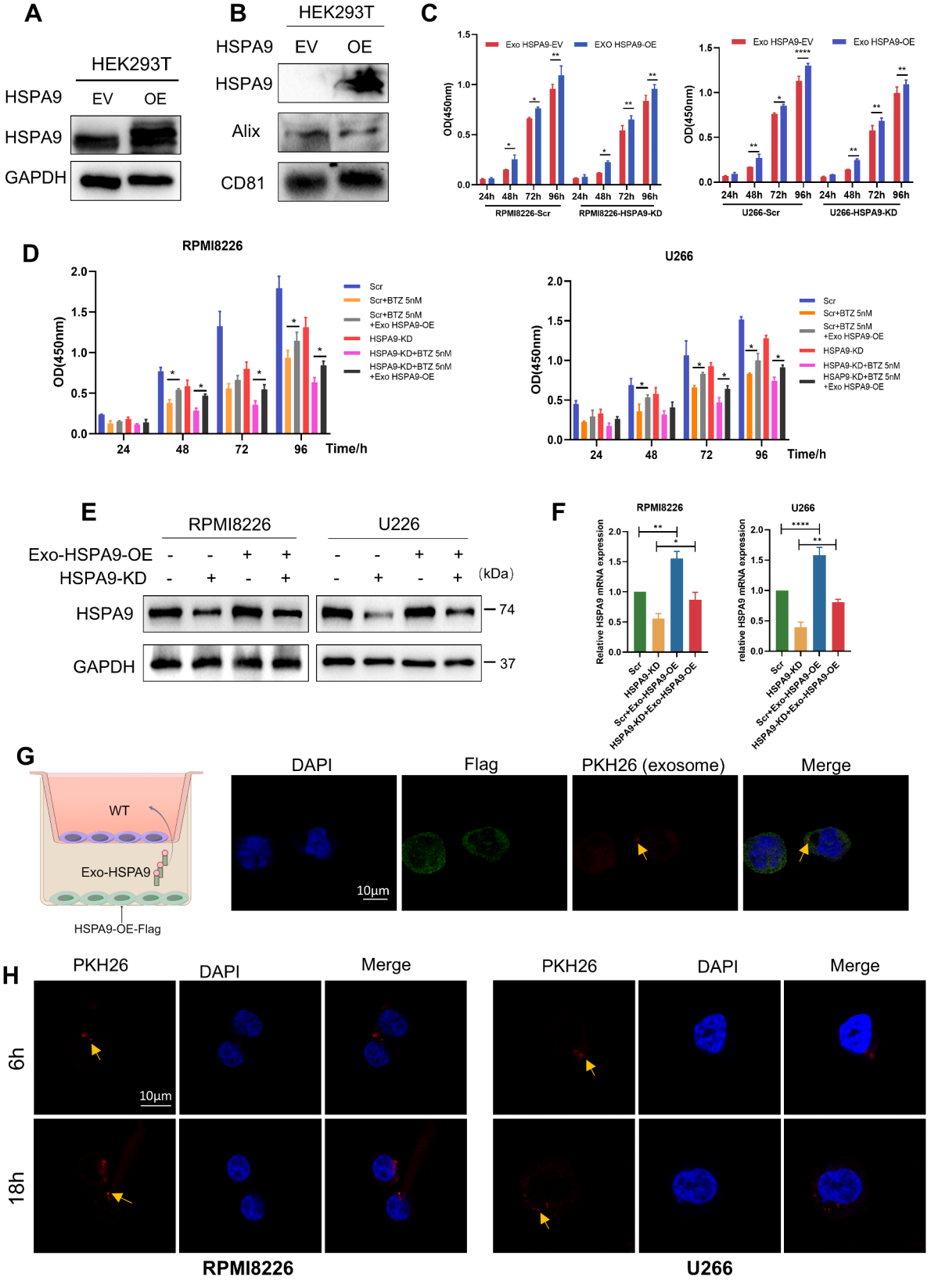

Fig. 3 (See legend on next page.)

(See figure on previous page.)

Fig. 3 Exosomes HSPA9 transferred from BTZ-resistant cells to sensitive cells in MM. (**A**) WB was utilized to detect the efficiency of HSPA9-OE. (**B**) WB was utilized to detect the markers of exosomes in HEK293T-HSPA9-OE cells. (**C**) Exosome-derived HSPA9 reversed the inhibition of cell proliferation caused by HSPA9 knockdown in MM. (**D**) CCK-8 assay detected the cell growth curves of exosome HSPA9-OE inducing HSPA9-KD MM cells to regain BTZ resistance. (**E**) WB assay and (**F**) qRT-PCR assay were employed to evaluate the expression levels of HSPA9 after the addition of exosomes HSPA9 for 48 h (WB) or 24 h (qRT-PCR) in MM cells. (**G**) Schematic image by Figdraw. RPMI8226-HSPA9-OE-FLAG and RPMI8226-WT cells were co-cultured for 24 h, and PKH26-labeled endogenous exosomes HSPA9 were detected in RPMI8226-WT cells. DAPI labeled nucleus and Flag labeled cells. Yellow arrows indicated exosomes. Scale bar, 10 μm. (**H**) Representative images of internalization of PKH26-labeled exosomes HSPA9 in MM cells. Yellow arrows indicated exosomes. Scale bar, 10 μm. *$P < 0.05$; **$P < 0.01$; ***$P < 0.001$

U266-WT MM cells (Fig. 4H). To clarify the biological characteristics of TRIP13, IHC was performed and demonstrated a marked elevation of TRIP13 protein expression in bone marrow biopsy tissue from the clinical BTZ-resistant patients ($P = 0.047$) (Fig. 4I). Compared to the baseline, the GSE31161 database revealed that the TRIP13 expression was markedly higher in relapse MM patients ($P < 0.001$) (Fig. 4J). These findings indicated that HSPA9 positively regulated TRIP13 under physiological conditions in MM cells.

HSPA9 recruites the deubiquitinating enzyme USP1, regulating the protein stability of TRIP13 in MM cells

As a member of ubiquitin-proteasome system, the DUB specifically hydrolyzes ubiquitin molecules from proteins with ubiquitin links and reversely regulates the protein degradation process. However, HSPA9 does not have DUB activity, so it may inhibit the ubiquitination process and TRIP13 protein degradation by regulating the binding of DUB to TRIP13. We first used TMT-labeled quantitative proteomics to screen the DEPs between HSPA9-EV and HSPA9-OE in RPMI8226 cells, and identified the high expression of USP1, a member of the DUB family in HSPA9-OE cells ($P = 0.0205$) (Fig. 5A). GO enrichment analysis demonstrated that a total of 210 DEPs were identified to be significantly enriched in the regulation of protein ubiquitination pathway (GO:0031396) in the biological process term (BP). According to them, the HSPA9-OE group had 3 up-regulated and 27 down-regulated expression ($P < 0.01$), indicating that the overexpression of HSPA9 inhibited the ubiquitination process in MM cells (black dotted box displayed) (Fig. 5B) (black dotted box displayed). To authenticate this hypothesis, proteasome inhibitor MG132 was added to MM cells and the endogenous ubiquitination level was detected. The results showed that HSPA9 knockdown significantly increased the ubiquitination level in MM cells (Fig. 5C). Additionally, we conducted co-IP experiments using TRIP13 antibody in both HSPA9-KD and HSPA9-Scr MM cells to assess the difference in ubiquitination levels. The results demonstrated that the ubiquitination level of TRIP13 was significantly reduced in HSPA9-KD cells (Fig. 5D). This finding provides evidence supporting the functional association between HSPA9 and TRIP13. In addition, co-IP revealed that HSPA9 could directly bind to USP1 (Fig. 5E), and USP1 could interact with TRIP13 in RPMI8226 cells (Fig. 5F). Immunofluorescence analysis validated that although TRIP13 was distributed in both cytoplasm and nucleus, the HSPA9-USP1-TRIP13 complex mainly existed in the cytoplasm (Fig. 5G).

To determine whether TRIP13 is a direct substrate of USP1, we first evaluated the effect of ML323 (a specific USP1 inhibitor) on the expression and function of TRIP13 in MM cells. WB analysis showed that ML323 impaired cellular USP1 activity and downregulated the expression of TRIP13 in a dose-dependent manner. However, the upstream HSPA9 expression had no significant change (Fig. 5H). Next, we used cycloheximide (CHX) tracking analysis to determine whether HSPA9 could affect the stability of the TRIP13 protein. We found that the knockdown of HSPA9 significantly shortened the half-life of the TRIP13 protein (Fig. 5I). These results suggested that USP1 and HSPA9 have similar effects in maintaining the stability of the TRIP13 protein.

HSPA9 recruites USP1 to inhibit TRIP13 ubiquitination degradation and promotes BTZ resistance in MM

To further investigate the role of the HSPA9 protein in forming the HSPA9-USP1-TRIP13 complex, we designed the full-length (FL) HSPA9 and its truncated mutant with Myc-tag (Fig. 6A-B). They were co-transfected into HEK 293T cells along with the HA-USP1 and FLAG-TRIP13 plasmids. Co-IP and WB assay were employed to analyze the structural mutation, which demonstrated that the carboxyl-terminal (C-terminal) of the HSPA9 peptide binding domain (432–679 aa) contributed to the interaction between USP 1 and TRIP13 (Fig. 6C-E). Above all, HSPA9 promoted the ubiquitination process of MM cells through its amino-terminal (N-terminal) ATPase domain in vitro ubiquitination assay (Fig. 6F). In summary, the heat shock protein HSPA9 may provide a molecular platform for the interaction between USP1 and TRIP13 through its C-terminal, while using the N-terminal ATPase domain for ubiquitination and maintaining the stability of TRIP13 protein.

Subsequently, we co-cultured MM cells with exosome HSPA9 for 48 h to investigate its effect on the HSPA9/USP1/TRIP13 regulatory axis. Interestingly, the addition of exogenous exosome HSPA9 significantly reversed the reduced expression of the downstream signalling pathway proteins USP1 and TRIP13 caused by HSPA9 knockdown (Fig. 6G). Interestingly, it was more sensitive

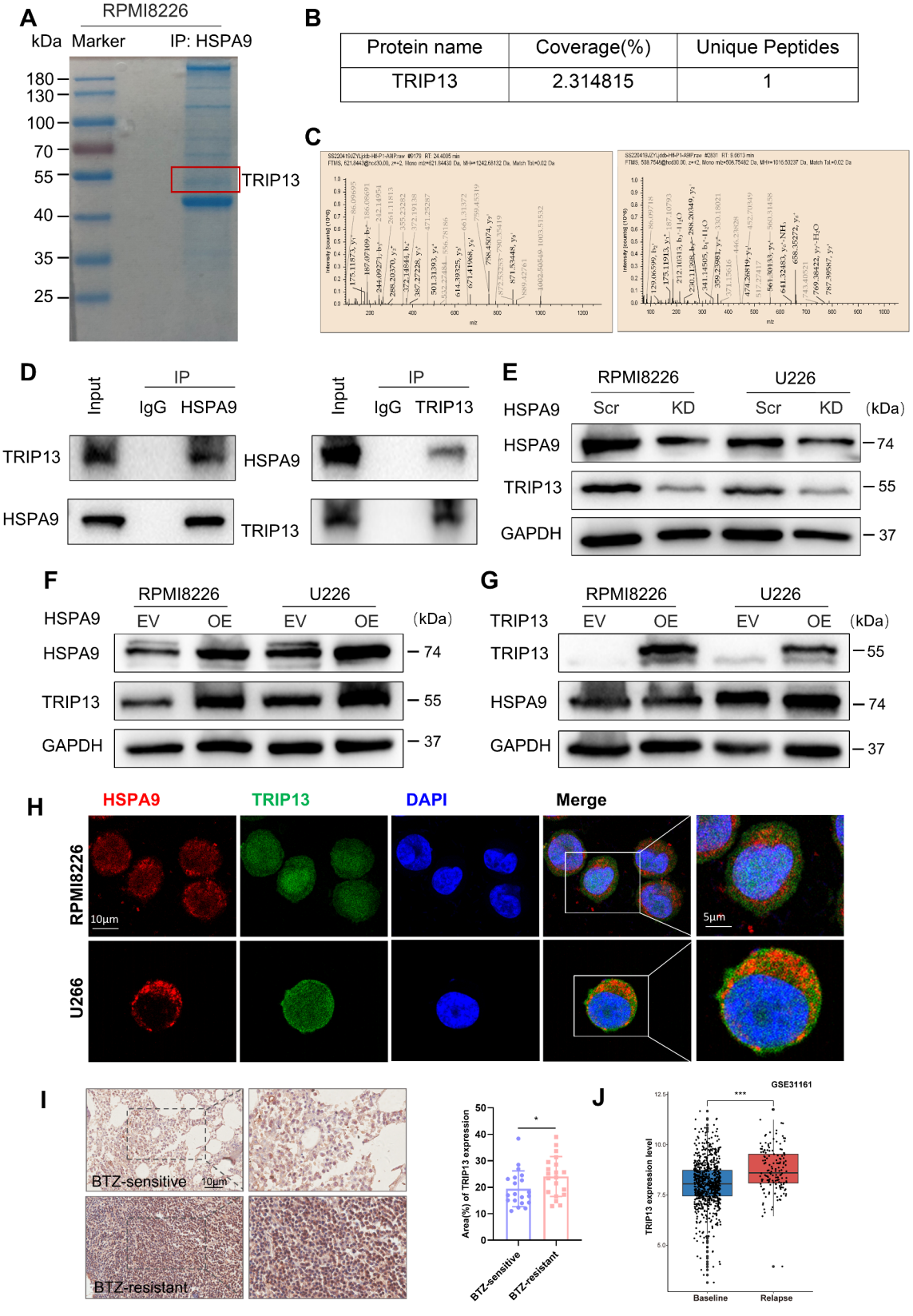

Fig. 4 (See legend on next page.)

(See figure on previous page.)

Fig. 4 HSPA9 positively regulates TRIP13 in MM. (**A**) SDS-PAGE and Coomassie Bright Blue (CBB) staining of HSPA9 immunoprecipitated proteins in RPMI8226-WT cell. The red box indicates the protein of interest. (**B**) The coverage, unique peptide count and (**C**) spectrum of TRIP13 were identified by IP-MS. (**D**) Co-IP assay was conducted to immunoblot HSPA9 and TRIP13 in RPMI8226 cells. The immunoblotting on the expression of HSPA9 and TRIP13 in (**E**) HSPA9-KD or (**F**) HSPA9-OE MM cells. (**G**) The immunoblotting on the expression of HSPA9 and TRIP13 in TRIP13-OE MM cells. (**H**) HSPA9 and TRIP13 were immunocolocalized in RPMI8226 and U266 cells. Scale bar, 10 μm. (**I**) IHC assay was used to detect the TRIP13 expression in bone marrow biopsies of MM patients ($P = 0.047$). (**J**) Compared to the baseline, the GSE31161 database showed that TRIP13 was highly expressed in relapse MM patients from the TT2 and TT3 regimens ($P < 0.001$). *$P < 0.05$; **$P < 0.01$; ***$P < 0.001$

to ML323 in HSPA9-KD MM cells (Fig. 6H). The rescue experiments found that USP1 or TRIP13 overexpressed could re-impart BTZ resistance in the RPMI-8226 and U266 HSPA9-KD MM cells (Fig. 6I-J). Taken together, these data suggest that HSPA9 interacts in a USP1-dependent manner and stabilizes TRIP13, thereby mediating BTZ resistance. Inhibiting the expression of the HSPA9-USP1-TRIP13 complex can overcome BTZ resistance in *vitro*.

Exosomes HSPA9 promote MM proliferation and BTZ resistance in, vivo

To evaluate the role of exosomes HSPA9 and the HSPA9-USP1-TRIP13 complex in vivo, we validated them in a xenograft mouse model for further exploration. Firstly, we constructed a xenograft tumor model in BALB/c nude mice through injecting RPMI8226 cells. PKH26-labeled exosomes HSPA9 were injected into mice through the tail vein, and then we evaluated the metabolic efficiency of exosomes HSPA9 through systemic circulation at different times after injection. Quantitative luminescence results showed that the concentration of exosomes in mice decreased gradually over time. Besides, the exosomes HSPA9 were still present at a high concentration in mice after injection for 48 h, and were distributed throughout the whole body (Fig. 7A).

To test the effect of BTZ or ML323 inhibitor on tumor, and whether adding exosomes HSPA9 could reverse tumor growth inhibition, mice were treated with BTZ or ML323 in the presence or absence of exosomes HSPA9. The data showed a significant reduction in the tumor weight and volume after treatment with BTZ and ML323 in comparison to the control group. Surprisingly, tumor weight and volume could be reversed after the addition of exosomes. However, no significant change was noted in the weight of the mice (Fig. 7B-E). IHC staining of representative tumors was used to detect the pathological condition of the tumor after drug treatment. Notably, mice administered exosomes HSPA9 in combination with BTZ or ML323 had higher level expressions of HSPA9 and Ki-67 than those treated with BTZ or ML323 alone (Fig. 7F). These results are consistent with our observations in *vitro*, suggesting that the HSPA9-USP1-TRIP13 complex is crucial for promoting the growth of MM, and the exosomes HSPA9 can confer BTZ resistance in vivo (Fig. 7G).

Discussion

As the backbone therapeutic agents of MM, PIs exemplified by BTZ, are incorporated into the majority of chemotherapy regimens. Despite the advancing therapeutic approaches and a median survival of more than seven years, MM remains an intractable disease. The current medical landscape has significant challenges in the management of MM relapse and PIs drug resistance [32, 33]. Therefore, a more comprehensive understanding of the basis for the involvement in MM resistance will help provide novel insights to combat MM effectively.

The characteristics of tumor cells and their interaction with the microenvironment drive the generation of drug resistance and progression in MM [34, 35]. Previous evidence suggests that the mechanism of bortezomib resistance may be related to an imbalance of the ubiquitin-proteasome system, endoplasmic reticulum stress, overexpression of heat shock proteins and changes in the tumor microenvironment. However, the molecular pathogenesis of bortezomib resistance in MM has not been not fully clarified, which brings difficulties in clinical treatment. Exosomes are essential components of intercellular communication in the tumor microenvironment. Several studies have proposed that exosomes play a critical role in drug chemotherapy resistance of various tumors [36–38]. Xu et al. [39] observed that exosomes released by mesenchymal stem cells could enhance the resistance to PIs by transmitting PSMA3 and PSMA3-AS1 in MM. Nevertheless, there is a paucity of research on the role of exosomes in drug resistance of myeloma cells. In this study, we extracted serum exosomes from

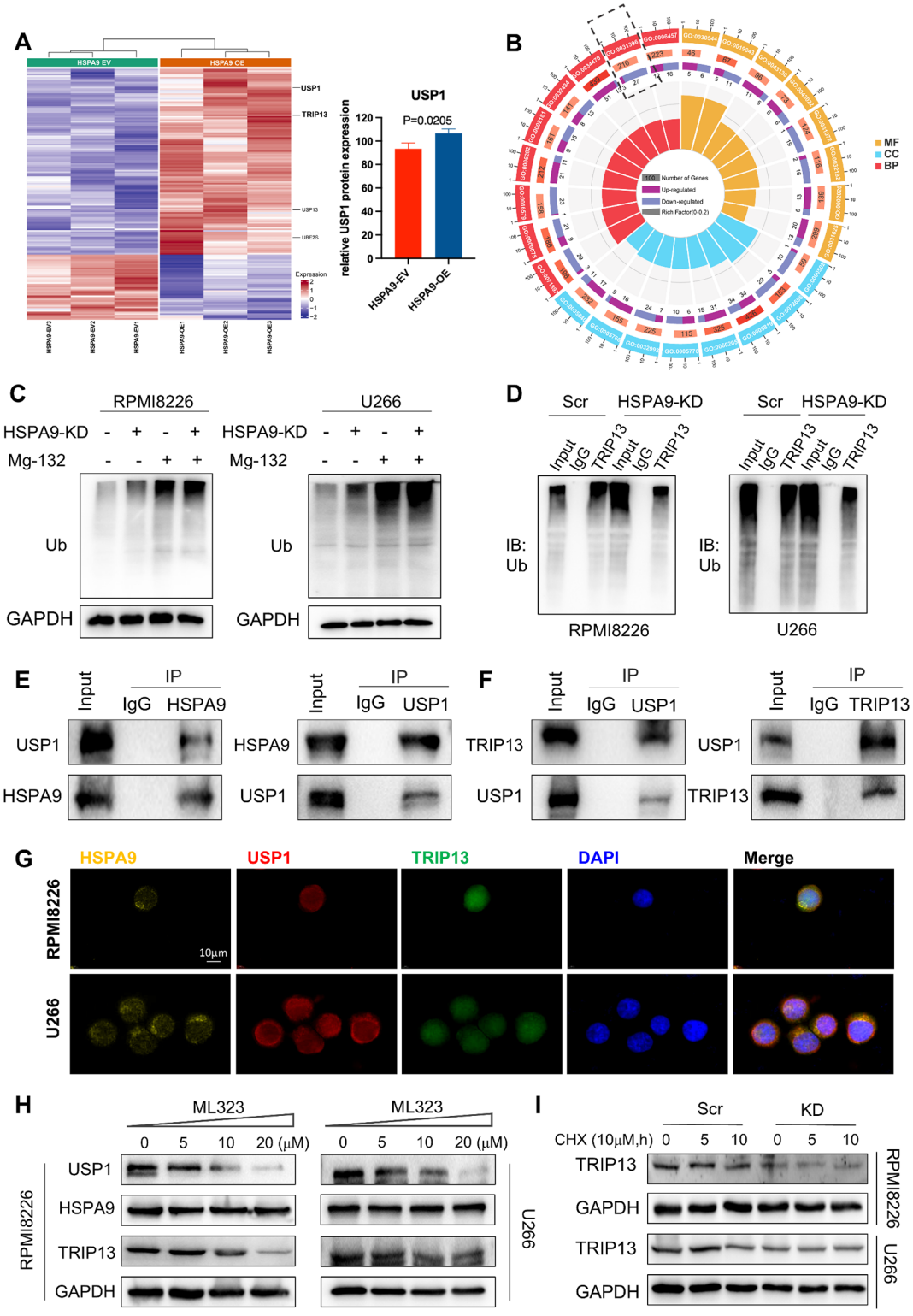

Fig. 5 (See legend on next page.)

(See figure on previous page.)

Fig. 5 HSPA9-USP1 interacts with TRIP13 in the cytoplasm. (**A**) The heatmaps and the relative expression of USP1 protein were shown in RPMI8226 (HSPA9-EV and HSPA9-OE) cells ($P = 0.0205$). (**B**) Twenty-five significantly enriched GO terms were shown from the outside to the inside. The first circle indicated the 25 enriched pathways. The second circle indicated the number and *P*-value of background proteins, and the length of the bar was in proportion to the quantity of protein. The third circle indicated the number of the DEPs in this pathway. The fourth circle indicated the value of rich factor in each pathway ($P < 0.01$). (**C**) WB assay detected that the knockdown of HSPA9 increased the ubiquitination level. (**D**) Co-IP assay using TRIP13 antibody detected that the ubiquitination level in MM cells. (**E**) Co-IP assay was performed on HSPA9 bound to USP1 in RPMI8226 cells. (**F**) Co-IP assay showed USP1 interacted with TRIP13 in RPMI8226 cells. (**G**) Immunofluorescence assay revealed that the HSPA9-USP1-TRIP13 complex was co-localized in the cytoplasm of MM cells. Scale bar, 10 μm. (**H**) WB assay on the expression of HSPA9, USP1 and TRIP13 exposed to different concentrations of ML323 for 24 h in MM cells. (**I**) WB assay on the expression of HSPA9, USP1 and TRIP13 exposed to CHX at different times in MM cells

MM patients and conducted a protein profiling analysis to investigate the potential upregulation of exosomes HSPA9 in BTZ-resistant MM patients. We found significantly high expression of exosomes HSPA9 in bortezomib-resistant MM cell lines. It was hypothesized that exosomes HSPA9 were closely related to MM bortezomib resistance.

HSPA9 is typically expressed at low levels in vivo, whereas it is inducibly expressed in various tumors and is associated with poor prognosis. Nevertheless, its function in MM has been infrequently documented. A review of public databases revealed that high expression of HSPA9 was linked to BTZ resistance and the progression of MM, as well as poor prognosis [40–42]. Combined with the IHC analysis of bone marrow tissues from MM patients in our center, the expression level of HSPA9 in tumor cells of BTZ-resistant patients was significantly higher than that of BTZ-sensitive patients. Subsequently, phenotype-related experiments also proved that HSPA9 could promote MM cell proliferation, BTZ resistance and stemness characteristics. Research shows that exosomes can transfer information between tumor cells and various cells in the microenvironment. Our data in vitro confirmed the role of exosomes HSPA9 in transmitting MM resistance. BTZ-resistant cells with high expression of HSPA9 can be packaged into exosomes, which are taken up by bortezomib-sensitive cells through endocytosis. This process allows the emergence of resistance in non-resistant cells, causing the transmission of BTZ resistance.

TRIP13 has been reported could facilitate multiple intracellular processes such as cancer proliferation, metastasis and drug resistance through homologous recombination repair and non-homologous end-junction DNA repair [43, 44]. Li Xu et al. [30] found that TRIP13 was overexpressed in BTZ-resistant MM cells. In turn, elevated TRIP13 expression promoted BTZ resistance in MM cells. However, the precise manner in which exosomes HSPA9 participate in the molecular signaling pathway of PTM through TRIP13, and its role in MM resistance remains largely unknown. To further explore the mechanism of HSPA9 mediating bortezomib resistance, we identified TRIP13 as the binding protein and the downstream target of HSPA9 through IP-MS. Immunofluorescent localization experiments further confirmed that the HSPA9-TRIP13 protein complex was mainly deposited in the MM cytoplasm. Although TRIP13 was expressed in both the cytoplasm and nucleus, it suggests that there might be an unidentified mechanism that promoted TRIP13 transportation from the nucleus to the cytoplasm, resulting in the HSPA9-TRIP13 protein complex being mainly deposited in the MM cytoplasm. Taken together, these findings collectively indicated that HSPA9 acted as a molecular chaperone for TRIP13 in MM cells.

Deubiquitination enables the selective degradation of proteins labeled with ubiquitin molecules [45] and plays a core role in a wide range of biological processes [46, 47]. However, the relationship between HSPA9-TRIP13 and DUB remains unknown. In this study, we elucidated that HSPA9 knockdown facilitated the ubiquitination of MM cells. It was of particular significance that HSPA9, functioning as a molecular chaperone, recruited USP1 to TRIP13 via its C-terminal domain. The N-terminal domain, in turn, provided the active site of the ubiquitination ATPase, thereby impeding the degradation of the TRIP13 protein. This evidence substantiates the proposition that the C-terminal domain of HSPA9 is indispensable for its engagement with USP1 and TRIP13 in MM cells. These results provide evidence that maintaining the stability of the TRIP13 protein depends on different structures in the HSPA9 proteome.

Consequently, our preclinical studies underscore that exosomes HSPA9 are secreted by bortezomib-resistant MM cells and taken up by bortezomib-sensitive MM cells through the endocytosis pathway. After entering the cells, HSPA9 binds USP1 and TRIP13 to form the HSPA9-USP1-TRIP13 complex, which is mainly deposited in the MM cytoplasm. This process directly transmits the resistance phenotype to bortezomib-sensitive cells. It transforms them into bortezomib-resistant cells, thereby facilitating the proliferation of MM cells, contributing to bortezomib resistance and reprogramming stemness

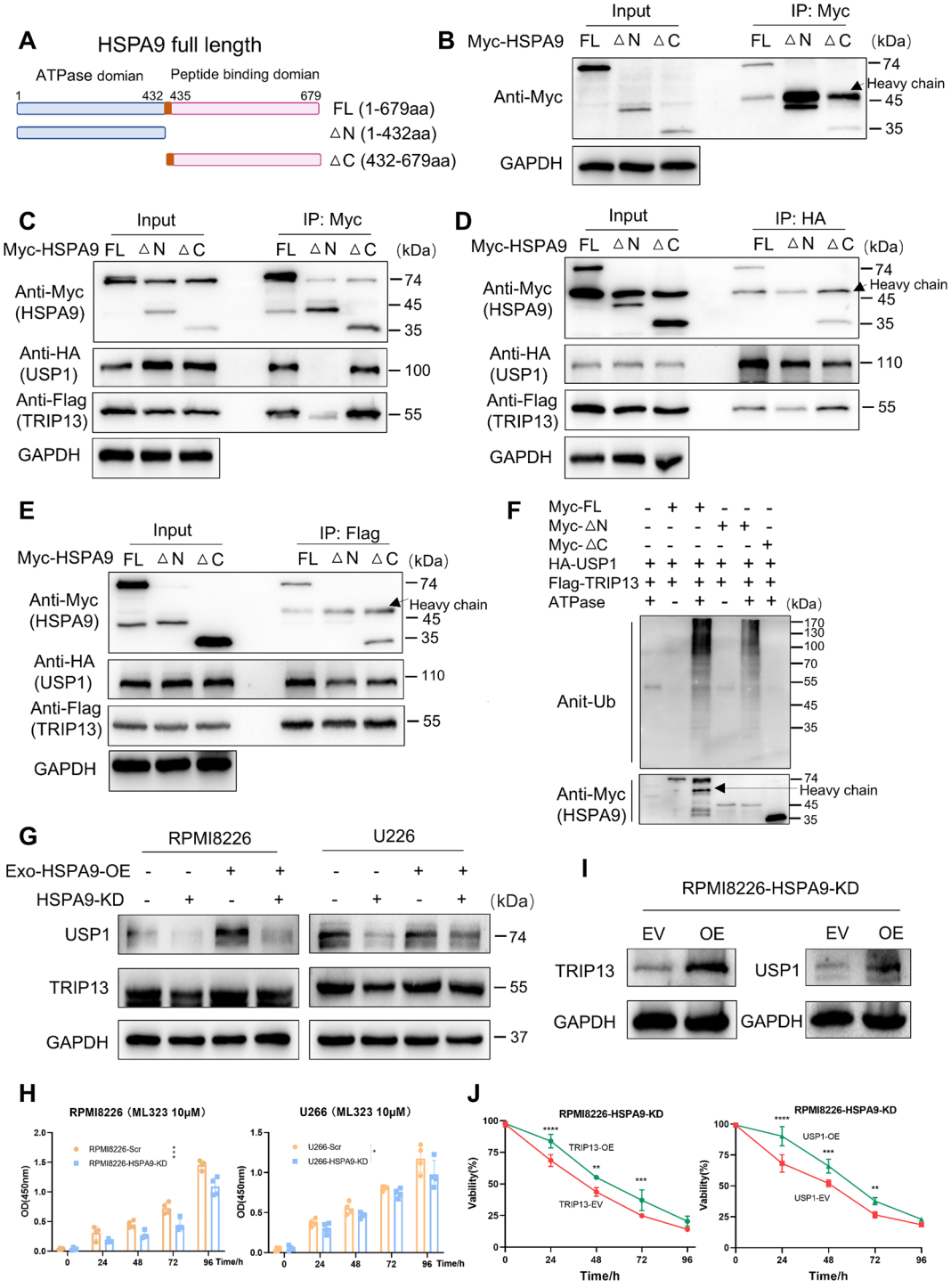

Fig. 6 HSPA9 recruits USP1 and regulates the stability of TRIP13 protein. (**A**) The full-length (FL) and truncated mutants of HSPA9 were modified with Myc-tag in the schematic image. (**B**) Co-IP assay was used to verify transfection efficacy using Myc-tag antibody in HEK293T cells. (**C**-**E**) Myc-HSPA9, HA-USP1 and FLAG-TRIP13 were co-transfected into HEK293T cells for 48 h. Co-IP assay and WB were performed with Myc-tag, HA-tag and Flag-tag antibody beads, respectively. (**F**) In vitro ubiquitination was performed using HSPA9 purified protein according to the reagent procedure. (**G**) WB assay was employed to evaluate the expression levels of USP1/TRIP13 after the addition of exosomes HSPA9 into MM cells for 48 h. (**H**) Treated with ML323 (10μM) for 96 h, the CCK-8 assay detected the cell viability in HSPA9-KD MM cell lines. (**I**) Overexpressing TRIP13 and USP1 in RPMI8226 HSPA9-KD cells, WB assay was assessed to measure the efficiency. (**J**) Treated with the BTZ (5nM) for 96 h, CCK-8 was used to evaluate the cell viability in HSPA9-KD MM cell lines. *$P < 0.05$; **$P < 0.01$; ***$P < 0.001$

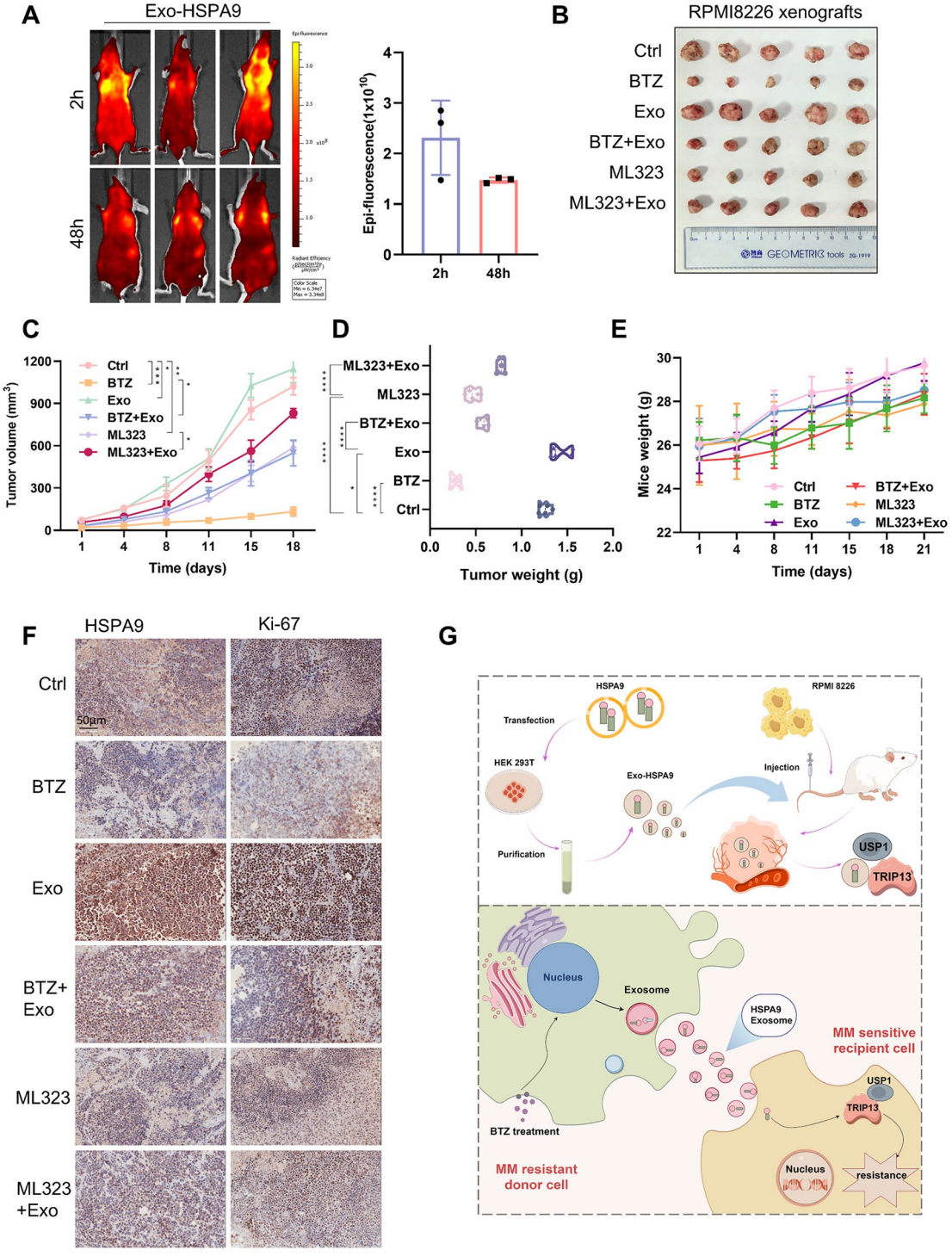

Fig. 7 Exosomes HSPA9 promote MM proliferation and BTZ resistance in vivo. (**A**) With PKH26-labeled exosomes HSPA9 (30 μg/mouse) injected into the Balb/c nude mice tail vein, quantitative luminescence was performed to evaluate the metabolic efficiency of exosomes HSPA9. RPMI8226 cell xenografts mice were treated with different drugs, including exosomes HSPA9. Representative images of (**B**) tumor image, (**C**) tumor volume, (**D**) tumor weight, (**E**) and mice weight were shown. (**F**) Representative images of HSPA9 and Ki67 IHC analysis were shown. Scale bar, 50 μm. (**G**) The molecular model mechanism of this study by Figdraw. *$P < 0.05$; **$P < 0.01$; ***$P < 0.001$; ****$P < 0.0001$

signature. In light of these findings, the advancement of small-molecule drugs targeting HSPA9 unravels a promising avenue for the therapy of BTZ resistance in MM.

Supplementary Information

The online version contains supplementary material available at https://doi.org/10.1186/s12964-025-02158-3.

Supplementary Material 1

Acknowledgements
Not applicable.

Author contributions
MS, and LC designed and conceived the study; MS, NS, and LC supervised the study; MS, NS, XL, and JY performed the experiments and analyzed the data; XS, YC and YX provided advice and technical assistance; and MS wrote the manuscript. All the authors contributed to and approved the final manuscript.

Funding
This work was supported by the National Natural Science Foundation of China (No. 82070223); Natural Science Foundation of Jiangsu Province (No. BK20241119); Social Development Project of Jiangsu Science and Technology Plan (No. BK20220718).
Data availbility: All data analyzed during the study are available from the corresponding author on reasonable request. The data can be found in the ProteomeXchange Consortium: PXD061782.

Data availability
No datasets were generated or analysed during the current study.

Declarations

Ethics approval and consent to participate
The animal experiments are approved by the institutional review committee of Nanjing Medical University (No. IACUC-2201011). This study was conducted following the Declaration of Helsinki and was approved by the Institutional Review Board of the First Affiliated Hospital of Nanjing Medical University Ethics Committee (No. 2021-SR-135). Informed consents were obtained from all participants.

Consent for publication
Not applicable.

Competing interests
The authors declare no competing interests.

Author details
[1]Department of Hematology, The First Affiliated Hospital of Nanjing Medical University, Jiangsu Province Hospital, Nanjing 210029, China

Received: 29 December 2024 / Accepted: 14 March 2025
Published online: 26 March 2025

References

1. Silberstein J, Tuchman S, Grant SJ. What Is Multiple Myeloma? JAMA. 2022;327(5):497.
2. Kumar SK, Callander NS, Adekola K, Anderson LJ, Baljevic M, Baz R, Campagnaro E, Castillo JJ, Costello C, D'Angelo C, et al. Multiple myeloma, version 2.2024, NCCN clinical practice guidelines in oncology. J Natl Compr Canc Netw. 2023;21(12):1281–301.
3. Poos AM, Prokoph N, Przybilla MJ, Mallm JP, Steiger S, Seufert I, John L, Tirier SM, Bauer K, Baumann A, et al. Resolving therapy resistance mechanisms in multiple myeloma by multiomics subclone analysis. Blood. 2023;142(19):1633–46.
4. Yu Z, Wei X, Liu L, Sun H, Fang T, Wang L, Li Y, Sui W, Wang K, He Y, et al. Indirubin-3'-monoxime acts as proteasome inhibitor: therapeutic application in multiple myeloma. EBioMedicine. 2022;78:103950.
5. Kozalak G, Butun I, Toyran E, Kosar A. Review on bortezomib resistance in multiple myeloma and potential role of emerging technologies. Pharmaceuticals (Basel). 2023; 16(1):111–132.
6. Hsu YL, Hung JY, Chang WA, Lin YS, Pan YC, Tsai PH, Wu CY, Kuo PL. Hypoxic lung cancer-secreted Exosomal miR-23a increased angiogenesis and vascular permeability by targeting Prolyl hydroxylase and tight junction protein ZO-1. Oncogene. 2017;36(34):4929–42.
7. Shao H, Chung J, Lee K, Balaj L, Min C, Carter BS, Hochberg FH, Breakefield XO, Lee H, Weissleder R. Chip-based analysis of Exosomal mRNA mediating drug resistance in glioblastoma. Nat Commun. 2015;6:6999.
8. Shi P, Li Y, Guo Q, Circular. RNA circPIP5K1A contributes to cancer stemness of osteosarcoma by miR-515-5p/YAP axis. J Transl Med. 2021;19(1):464.
9. Liu X, Guo Q, Gao G, Cao Z, Guan Z, Jia B, Wang W, Zhang K, Zhang W, Wang S, et al. Exosome-transmitted circCABIN1 promotes Temozolomide resistance in glioblastoma via sustaining erbb downstream signaling. J Nanobiotechnol. 2023;21(1):45.
10. Wu Q, Zhou L, Lv D, Zhu X, Tang H. Exosome-mediated communication in the tumor microenvironment contributes to hepatocellular carcinoma development and progression. J Hematol Oncol. 2019;12(1):53.
11. Wang X, Huang J, Chen W, Li G, Li Z, Lei J. The updated role of Exosomal proteins in the diagnosis, prognosis, and treatment of cancer. Exp Mol Med. 2022;54(9):1390–400.
12. Wu Y, Zhu X, Shen R, Huang J, Xu X, He S. miR-182 contributes to cell adhesion-mediated drug resistance in multiple myeloma via targeting PDCD4. Pathol Res Pract. 2019;215(11):152603.
13. Shah SP, Lonial S, Boise LH. When cancer fights back: multiple myeloma, proteasome Inhibition, and the Heat-Shock response. Mol Cancer Res. 2015;13(8):1163–73.
14. Ferguson ID, Lin YT, Lam C, Shao H, Tharp KM, Hale M, Kasap C, Mariano MC, Kishishita A, Patino EB, et al. Allosteric HSP70 inhibitors perturb mitochondrial proteostasis and overcome proteasome inhibitor resistance in multiple myeloma. Cell Chem Biol. 2022;29(8):1288–e13027.
15. Kambhampati S, Wiita AP. Lessons Learned from Proteasome Inhibitors, the Paradigm for Targeting Protein Homeostasis in Cancer. Adv Exp Med Biol. 2020;1243:147–62.
16. Kabakov AE, Gabai VL. HSP70s in Breast Cancer: Promoters of Tumorigenesis and Potential Targets/Tools for Therapy. Cells. 2021; 10(12):3446–3489.
17. Wu PK, Hong SK, Starenki D, Oshima K, Shao H, Gestwicki JE, Tsai S, Park JI. Mortalin/HSPA9 targeting selectively induces KRAS tumor cell death by perturbing mitochondrial membrane permeability. Oncogene. 2020;39(21):4257–70.
18. Ding P, Ma Z, Fan Y, Feng Y, Shao C, Pan M, Zhang Y, Huang D, Han J, Hu Y, Yan X. Emerging role of ubiquitination/deubiquitination modification of PD-1/PD-L1 in cancer immunotherapy. Genes Dis. 2023;10(3):848–63.
19. Snyder NA, Silva GM. Deubiquitinating enzymes (DUBs): Regulation, homeostasis, and oxidative stress response. J Biol Chem. 2021;297(3):101077.
20. Vaithiyanathan M, Yu Y, Rahnama A, Pettigrew JH, Safa N, Liu D, Gauthier TJ, Floyd ZE, Melvin AT. Characterization of PMI-5011 on the Regulation of Deubiquitinating Enzyme Activity in Multiple Myeloma Cell Extracts. Biochem Eng J. 2021; 166:107834–107859.
21. Huang P, Wang Y, Zhang P, Li Q. Ubiquitin-specific peptidase 1: assessing its role in cancer therapy. Clin Exp Med. 2023;23(7):2953–66.
22. Das DS, Das A, Ray A, Song Y, Samur MK, Munshi NC, Chauhan D, Anderson KC. Blockade of Deubiquitylating Enzyme USP1 Inhibits DNA Repair and Triggers Apoptosis in Multiple Myeloma Cells. Clin Cancer Res. 2017;23(15):4280–9.
23. Yuan P, Feng Z, Huang H, Wang G, Chen Z, Xu G, Xie Z, Jie Z, Zhao X, Ma Q, et al. USP1 inhibition suppresses the progression of osteosarcoma via destabilizing TAZ. Int J Biol Sci. 2022;18(8):3122–36.
24. Vader G. Pch2(TRIP13): controlling cell division through regulation of HORMA domains. Chromosoma. 2015;124(3):333–9.
25. Lu S, Guo M, Fan Z, Chen Y, Shi X, Gu C, Yang Y. Elevated TRIP13 drives cell proliferation and drug resistance in bladder cancer. Am J Transl Res. 2019;11(7):4397–410.
26. Lu S, Qian J, Guo M, Gu C, Yang Y. Insights into a Crucial Role of TRIP13 in Human Cancer. Comput Struct Biotechnol J. 2019;17:854–61.
27. Shaughnessy JJ, Zhan F, Burington BE, Huang Y, Colla S, Hanamura I, Stewart JP, Kordsmeier B, Randolph C, Williams DR, et al. A validated gene expression

model of high-risk multiple myeloma is defined by deregulated expression of genes mapping to chromosome 1. Blood. 2007;109(6):2276–84.
28. Zhou W, Yang Y, Xia J, Wang H, Salama ME, Xiong W, Xu H, Shetty S, Chen T, Zeng Z, et al. NEK2 induces drug resistance mainly through activation of efflux drug pumps and is associated with poor prognosis in myeloma and other cancers. Cancer Cell. 2013;23(1):48–62.
29. Li C, Xia J, Franqui-Machin R, Chen F, He Y, Ashby TC, Teng F, Xu H, Liu D, Gai D et al. TRIP13 modulates protein deubiquitination and accelerates tumor development and progression of B cell malignancies. J Clin Invest. 2021; 131(14):e146893–906.
30. Xu L, Wang Y, Wang G, Guo S, Yu D, Feng Q, Hu K, Chen G, Li B, Xu Z, et al. Aberrant activation of TRIP13-EZH2 signaling axis promotes stemness and therapy resistance in multiple myeloma. Leukemia. 2023;37(7):1576–9.
31. Rajkumar SV, Dimopoulos MA, Palumbo A, Blade J, Merlini G, Mateos M, Kumar S, Hillengass J, Kastritis E, Richardson P, et al. International Myeloma Working Group updated criteria for the diagnosis of multiple myeloma. Lancet Oncol. 2014;15(12):e538–48.
32. Tomlin FM, Gerling-Driessen U, Liu YC, Flynn RA, Vangala JR, Lentz CS, Clauder-Muenster S, Jakob P, Mueller WF, Ordonez-Rueda D, et al. Inhibition of NGLY1 Inactivates the Transcription Factor Nrf1 and Potentiates Proteasome Inhibitor Cytotoxicity. ACS Cent Sci. 2017;3(11):1143–55.
33. Bianchi G, Oliva L, Cascio P, Pengo N, Fontana F, Cerruti F, Orsi A, Pasqualetto E, Mezghrani A, Calbi V, et al. The proteasome load versus capacity balance determines apoptotic sensitivity of multiple myeloma cells to proteasome inhibition. Blood. 2009;113(13):3040–9.
34. Ni J, Bucci J, Malouf D, Knox M, Graham P, Li Y. Exosomes in Cancer Radioresistance. Front Oncol. 2019;9:869.
35. Zhuang J, Shirazi F, Singh RK, Kuiatse I, Wang H, Lee HC, Berkova Z, Berger A, Hyer M, Chattopadhyay N, et al. Ubiquitin-activating enzyme inhibition induces an unfolded protein response and overcomes drug resistance in myeloma. Blood. 2019;133(14):1572–84.
36. Chen T, Zhang G, Kong L, Xu S, Wang Y, Dong M. Leukemia-derived exosomes induced IL-8 production in bone marrow stromal cells to protect the leukemia cells against chemotherapy. Life Sci. 2019;221:187–95.
37. Lv MM, Zhu XY, Chen WX, Zhong SL, Hu Q, Ma TF, Zhang J, Chen L, Tang JH, Zhao JH. Exosomes mediate drug resistance transfer in MCF-7 breast cancer cells and a probable mechanism is delivery of P-glycoprotein. Tumour Biol. 2014;35(11):10773–9.
38. Zhou W, Fong MY, Min Y, Somlo G, Liu L, Palomares MR, Yu Y, Chow A, O'Connor ST, Chin AR, et al. Cancer-secreted miR-105 destroys vascular endothelial barriers to promote metastasis. Cancer Cell. 2014;25(4):501–15.
39. Xu H, Han H, Song S, Yi N, Qian C, Qiu Y, Zhou W, Hong Y, Zhuang W, Li Z, et al. Exosome-Transmitted PSMA3 and PSMA3-AS1 Promote Proteasome Inhibitor Resistance in Multiple Myeloma. Clin Cancer Res. 2019;25(6):1923–35.
40. Hanamura I, Huang Y, Zhan F, Barlogie B, Shaughnessy J. Prognostic value of cyclin D2 mRNA expression in newly diagnosed multiple myeloma treated with high-dose chemotherapy and tandem autologous stem cell transplantations. Leukemia. 2006;20(7):1288–90.
41. Mitchell JS, Li N, Weinhold N, Forsti A, Ali M, van Duin M, Thorleifsson G, Johnson DC, Chen B, Halvarsson BM, et al. Genome-wide association study identifies multiple susceptibility loci for multiple myeloma. Nat Commun. 2016;7:12050.
42. Driscoll JJ, Pelluru D, Lefkimmiatis K, Fulciniti M, Prabhala RH, Greipp PR, Barlogie B, Tai YT, Anderson KC, Shaughnessy JJ, et al. The sumoylation pathway is dysregulated in multiple myeloma and is associated with adverse patient outcome. Blood. 2010;115(14):2827–34.
43. Clairmont CS, Sarangi P, Ponnienselvan K, Galli LD, Csete I, Moreau L, Adelmant G, Chowdhury D, Marto JA. D'Andrea AD. TRIP13 regulates DNA repair pathway choice through REV7 conformational change. Nat Cell Biol. 2020;22(1):87–96.
44. Banerjee R, Russo N, Liu M, Basrur V, Bellile E, Palanisamy N, Scanlon CS, van Tubergen E, Inglehart RC, Metwally T, et al. TRIP13 promotes error-prone nonhomologous end joining and induces chemoresistance in head and neck cancer. Nat Commun. 2014;5:4527.
45. Chen S, Liu Y, Zhou H. Advances in the Development Ubiquitin-Specific Peptidase (USP) Inhibitors. Int J Mol Sci. 2021; 22(9):4546–74.
46. Qin W, Steinek C, Kolobynina K, Forne I, Imhof A, Cardoso MC, Leonhardt H. Probing protein ubiquitination in live cells. Nucleic Acids Res. 2022;50(21):e125.
47. Mevissen T, Komander D. Mechanisms of Deubiquitinase Specificity and Regulation. Annu Rev Biochem. 2017;86:159–92.

Publisher's note